

Sand particle-Induced deterioration of thermal barrier coatings on gas turbine blades

Muthuvel Murugan^{*1}, Anindya Ghoshal¹, Michael J. Walock¹, Blake D. Barnett¹,
Marc S. Pepi¹ and Kevin A. Kerner²

¹U.S. Army Research Laboratory, Building 4603, Aberdeen Proving Ground, Maryland 21005, U.S.A.

²Aviation Development Directorate, U.S. Army Aviation and Missile Research, Development and Engineering Center, Building 401, Fort Eustis, Virginia 23604, U.S.A.

(Received February 20, 2016, Revised April 27, 2016, Accepted May 9, 2016)

Abstract. Gas turbines operating in dusty or sandy environment polluted with micron-sized solid particles are highly prone to blade surface erosion damage in compressor stages and molten sand attack in the hot-sections of turbine stages. Commercial/Military fixed-wing aircraft engines and helicopter engines often have to operate over sandy terrains in the middle eastern countries or in volcanic zones; on the other hand gas turbines in marine applications are subjected to salt spray, while the coal-burning industrial power generation turbines are subjected to fly-ash. The presence of solid particles in the working fluid medium has an adverse effect on the durability of these engines as well as performance. Typical turbine blade damages include blade coating wear, sand glazing, Calcia-Magnesia-Alumina-Silicate (CMAS) attack, oxidation, plugged cooling holes, all of which can cause rapid performance deterioration including loss of aircraft. The focus of this research work is to simulate particle-surface kinetic interaction on typical turbomachinery material targets using non-linear dynamic impact analysis. The objective of this research is to understand the interfacial kinetic behaviors that can provide insights into the physics of particle interactions and to enable leap ahead technologies in material choices and to develop sand-phobic thermal barrier coatings for turbine blades. This paper outlines the research efforts at the U.S Army Research Laboratory to come up with novel turbine blade multifunctional protective coatings that are sand-phobic, sand impact wear resistant, as well as have very low thermal conductivity for improved performance of future gas turbine engines. The research scope includes development of protective coatings for both nickel-based super alloys and ceramic matrix composites.

Keywords: turbine blade coatings; thermal barrier coatings; sand particle glazing; gas turbine coating damage

1. Introduction

Thermal barrier coatings (TBCs) made of low-thermal conductivity ceramics are currently used in gas turbine engines to provide thermal insulation to nickel superalloy blades operating in hot gas stream. This allows increased turbine inlet temperature, thereby increasing engine efficiency and performance. In order to advance the gas turbine engine technology for future Army

*Corresponding author, Ph.D., E-mail: muthuvel.murugan.civ@mail.mil

helicopters, new blade materials, novel thermal barrier, and sand resistant coatings are continually being explored. The development of uncooled turbine blades and other hot section components will be enabled in gas turbines with the advent of new high temperature engine materials: e.g. Ceramic matrix composites (CMCs) and novel coating materials like pyrochlores, doped zirconia, hexa-aluminates, perovskites and aluminates (e.g., lanthanum-titanium-alumina oxide, lanthanum zirconate etc.). Increasing the turbine inlet temperature further with the advent of emerging high temperature materials such as CMCs and novel high temperature coatings can greatly enhance fuel efficiency, longer life, and increased power density of future military helicopter engines.

When discussing future Army aviation, increased operational effectiveness is one of the primary considerations to extend range and speed of military rotorcraft. This key requirement is dependent on the future development of advanced gas turbine engine technology. Specifically, new engines will have higher power densities and lower fuel requirements over existing technologies. In addition, the engines will be more damage tolerant enabling longer operating hours before required maintenance. To this end, new turbine blade materials and novel barrier coatings are continually being explored by industrial, academic, and government researchers. Enhancements in these areas will result in increased turbine inlet temperatures, which will enhance fuel efficiency and provide instantaneous additional power for extreme maneuvers of military aircraft. Fig. 1 illustrates the evolution of high temperature materials over the past few decades. Monolithic metallic components with good high temperature tolerance, creep strength and fracture toughness have been cost-effective solutions for high temperature demands. Further, intermetallics and single crystal materials such as nickel-based superalloys and Mo-based superalloys came into use with improved thermomechanical fatigue, higher melting points, and lower coefficient of thermal expansion (CTE). Thermal Barrier Coatings (TBCs) are used to achieve more effective thermal insulation in conjunction with cooling holes to keep surfaces within the safe operating temperature range of the material. Ceramic composites are emerging as advanced materials for high temperature applications as they have the potential to reduce, perhaps even eliminate, the need for conventional cooling mechanisms.

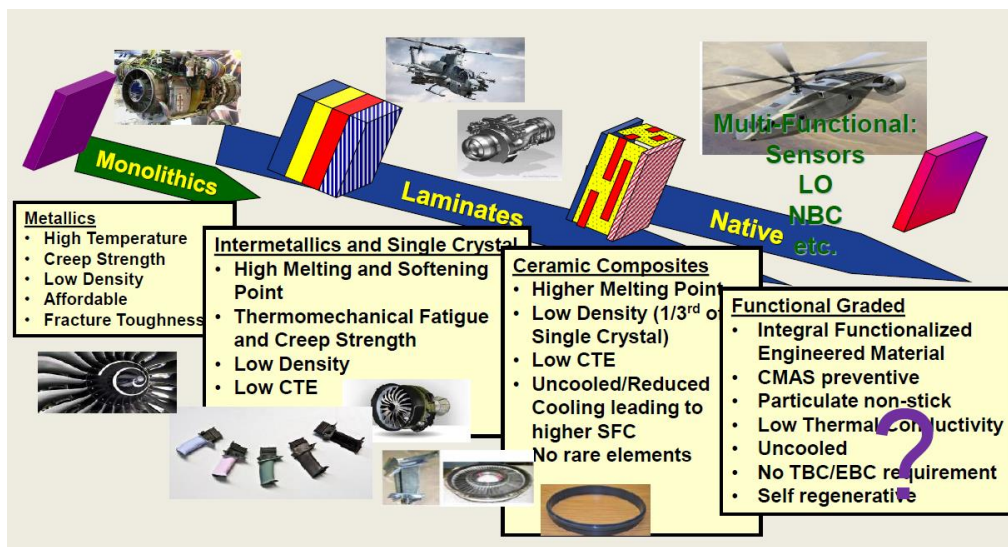


Fig. 1 The evolution of high temperature materials

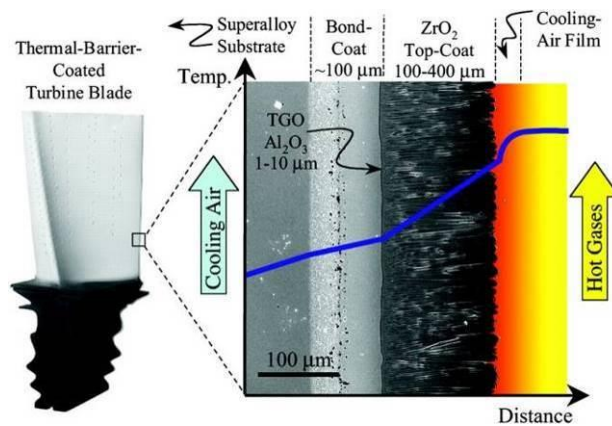


Fig. 2 Typical gas turbine blade consisting of a nickel-superalloy substrate with an intermetallic bond-coat, thermally-grown oxide, and the low thermal conductivity top-coat (Padture *et al.* 2002) (Reprinted with permission from AAAS)

Currently, the first-stage, high-pressure turbine blades can experience inlet temperatures in the range of 1400-1500°C. This is significantly higher than the previous generation engines. Modern engines are able to operate in this regime due to the development of advanced materials for the first-stage, high-pressure turbine. The structure of a typical turbine blade is described in the publication (Padture, Gell *et al.* 2002) and is shown in Fig. 2. A single-crystal, nickel-based superalloy forms the main blade substrate component. This is coated with an intermetallic bond-coat (about 100 μm thick), such as platinum/palladium-modified aluminides. The thermal barrier coating is yttria-stabilized zirconia (YSZ), and ranges from 150-400 μm in thickness (depending on the engine's application). During normal operations, a thin thermally grown oxide (TGO) layer forms between the bond-coat and the TBC. This prevents further oxidation of the bond-coat and superalloy substrate.

Another, recently adopted option is the replacement of the nickel superalloy with a ceramic matrix composite (CMC). The CMC can operate at significantly higher temperatures, and reduces the overall weight of the engine. An example structure consists of a SiC-SiC CMC, coated with a multilayer environmental barrier coating (EBC). The EBC layers consist of a barium strontium aluminum silicate (BSAS) top coat, an intermediate bond-coat (combination of mullite and BSAS), and a SiC seal coat over the CMC. In the Ni-based metallic turbine blade, the blades are actively cooled via pressurized air flowing through cooling holes. This need for cooling air may be eliminated with the use of CMC blades in future engines.

The development of novel barrier coatings (such as doped zirconia, pyrochlores, hexaaluminates, perovskites, and/or rare-earth doped aluminates) and functionally-graded CMC's will enable the use of lightweight, uncooled turbine blades. This can greatly enhance the fuel efficiency, the operating lifetime, and the power density of future military helicopter engines.

1.1 Damage effects due to sand particulates

Turbomachinery flows that contain sand, dust, and/or fly ash cause a vulnerable and often inescapable condition in certain environmental operating conditions. And while modern particle separators can remove the large particles (over 80 μm in size), fine particulates that get through,

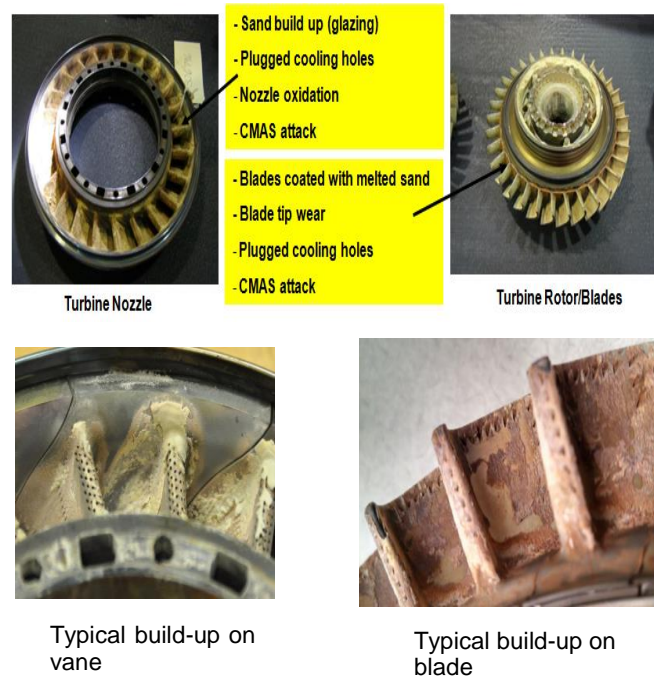


Fig. 3 Typical rotorcraft gas turbine engine nozzle and rotor blades with sand-induced damages



Fig. 4 Sand glazing deposits found on Gas Generator Turbine (GGT) hardware from field returned engines

can still be quite damaging. In addition to the blade degradation through normal erosive processes, the high inlet temperatures can cause the fine particles to undergo a phase change and become molten (Smialek, Archer *et al.* 1994, Borom, Johnson *et al.* 1996). This can lead to sand glazing, blade tip wear, calcia-magnesia-alumina-silicate (CMAS) attack, oxidation, and plugged cooling holes, all of which can cause rapid performance deterioration (Fig. 3).

Field-returned engines from Army rotorcraft operating in Southwest Asia (SWA) show a significant number of occurrences of CMAS related damages (Fig. 4). Army Rotorcraft Engines are being pulled out of service at a substantial knockdown on the design life. Novel TBCs which are also resistant to particle impact and sand-induced surface degradation can greatly reduce the vulnerability of engines operating in hostile particle-laden environments.

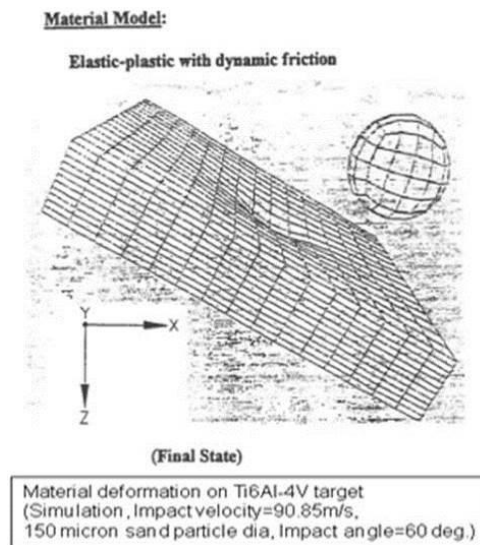


Fig. 5 Particle-target plate impact model

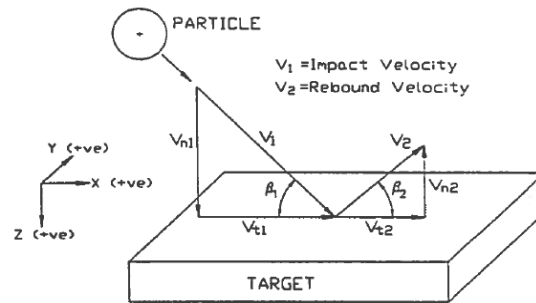
2. Particle-surface interaction model

While there are significant efforts to solve this sand problem through experimentation (Levi, Hutchinson *et al.* 2012, Kramer, Yang *et al.* 2008, Rai, Bhattacharya *et al.* 2010, Aygun, Vasiliev *et al.* 2007, Drexler, Shinoda *et al.* 2010b), there have been surprisingly few attempts to model the process (Evans, Mumm *et al.* 2001, Hutchinson and Evans 2002) and gain a physio-chemical understanding of the problem. Most previous research efforts have focused on studying the rebound characteristics of particles impacting turbomachinery materials at high speed and developing semi-empirical models of the erosion (Tabakoff 1991, Hamed 1988). Typically, this is done with a spherical quartz particle impacting a flat target (made of typical turbomachinery materials) with nonlinear dynamic impact analysis software, such as DYNA3D (LSTC 2007). In a previous modeling effort, conducted by researchers at the University of Cincinnati (Murugan, Tabakoff *et al.* 1994), a finite-element model, as shown in Fig. 5, was developed to study the particle impact rebound characteristics, and then these parameters were used to predict surface damage and erosion.

The restitution characteristics from this particle kinematics model and laser based measurements (Murugan, Tabakoff *et al.* 1994, Tabakoff, Murugan *et al.* 1994) were used to determine erosion rates on various compressor and turbine blade materials. The particle restitution characteristic parameters are defined in Fig. 6 (Murugan, Tabakoff *et al.* 1994, Tabakoff, Murugan *et al.* 1994).

2.1 Computational model

Since the interactions of ultra-fine particles on turbine blades are complex, multi-physics phenomena that include dynamic mechanical impact, thermal elements and chemical reactions, a multi-scale approach is currently being under-taken at the U.S Army Research Laboratory (ARL) to study the hot-section turbine blade surface deterioration. This scheme includes dynamic



Definitions of Restitutive Coefficients

Total Velocity Restitution Ratio,	$e_V = V_2/V_1$
Directional Restitution Ratio,	$e_\beta = \beta_2/\beta_1$
Tangential Velocity Restitution Ratio,	$e_t = V_{t2}/V_{t1}$
Normal Velocity Restitution Ratio,	$e_n = V_{n2}/V_{n1}$

Fig. 6 Definitions of the impact model's particle restitution characteristics

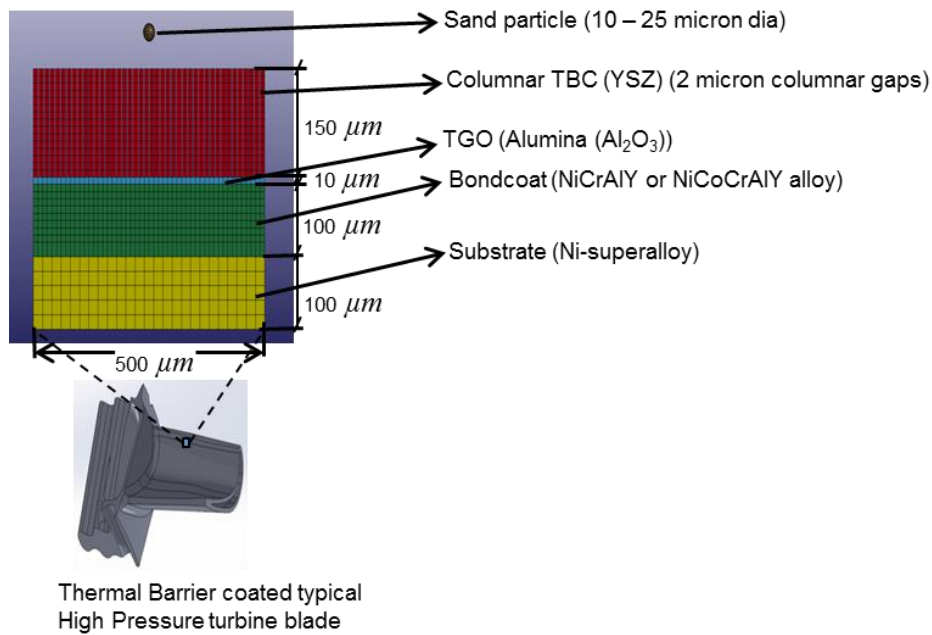


Fig. 7 Microstructure dynamic particle-surface impact model

mechanical impact simulations, thermal effects, computational fluid dynamics, and atomistic scale models in order to have comprehensive multi-physics based computations.

Building upon the prior work described above, the thermo-mechanical models will elucidate the impact dynamics and related effects on the TBC. As a first-step, the model details the impact of

a spherical sand particle on a relevant coating microstructure. Using nonlinear dynamic impact analysis software (LS-DYNA), a multi-layer structure was created with a highly refined mesh of $10\ \mu\text{m} \times 5\ \mu\text{m} \times 5\ \mu\text{m}$ (Fig. 7). Tied contact algorithms were used at the material interfaces. Published material data were used for the four layers with a material model of Mat-Plastic available in the LS-DYNA solver (LSTC 2007). A Surface-to-Surface contact algorithm, available in the software, was utilized for particle contact with the columnar TBC (LSTC 2007) that has inter-columnar gaps of $2\ \mu\text{m}$. In future computations, the model will be enhanced with information from complementary modeling techniques, surface morphology characterization, and experimental results.

In parallel with the dynamic mechanical impact model, computational fluid dynamics (CFD) simulations will investigate the flow of fine and ultra-fine particles in a relevant fluid of hot, combusted gases. This will provide the necessary velocities and particle trajectories to efficiently, and accurately calculate the particle impact statistics on different regions of the rotors and stators of the high-pressure turbine. Atomistic modeling efforts will center on several aspects of the degradation process. With information from dynamic impact mechanical and thermal/CFD models, kinetic Monte Carlo simulations will describe the “growth” of any contaminant CMAS buildup. This information will guide the refinement of a micro-scale diffusion model, developed in COMSOL Multiphysics (which is a finite-element based code). As the contaminant buildup (sand glazing) grows and solidifies, it diffuses into the voids and grain boundaries of the TBC (Levi, Hutchinson *et al.* 2012). The length scale of this diffusion can have significant effects on the failure mechanisms involved in CMAS degradation of hot section components. Coupled to this effort, molecular dynamics (MD) simulations will investigate the relevance of chemical reactions between the ultra-fine CMAS contaminants and the TBC. The rate/type of reactions may affect the diffusion kinetics modeled in COMSOL. In addition, MD code may reveal crystallographic phase changes in the relevant materials. Stresses induced by these phase changes can also affect the component failure mechanisms. It should be noted that many state-of-the-art computational materials models involve few elements/molecules and only one or two relevant environmental parameters. With this multi-level approach, researchers at ARL are attempting to overcome the technical challenges involved in this multi-physics based material damage phenomena.

2.2 Modeling results

The numerical solution of this first dynamic impact mechanical model provides stresses, strains, deformations etc., and includes the velocity history during particle-surface impact interactions. The explicit computations were terminated after the particle reached an approximately steady rebound velocity. For the results shown here, the particle was assumed spherical in shape, with a diameter of $25\ \mu\text{m}$. The initial particle velocity was $200\ \text{m/s}$ (~ 0.6 Mach) with an impact angle of 45° , with respect to the surface. The model is setup to run with different particle diameters, particle velocities, and impact angles to conduct simulations at different conditions and study the extent of TBC surface damage.

The particle velocity time history for $25\ \mu\text{m}$ diameter sand particle is shown in Fig. 8. The figure shows that after impact the particle velocity is reduced by approximately 50%. A considerable amount of the particle’s kinetic energy is absorbed by the TBC during each particle impact. In Fig. 9, significant plastic strains are observed on the surface of the columnar TBC due to single sand particle impact. Over multiple impacts, considerable strain on the TBC will accumulate and may eventually damage the TBC.

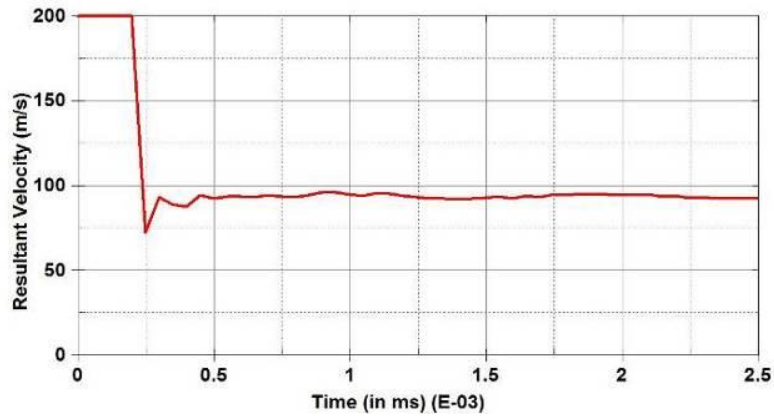


Fig. 8 Particle velocity change during surface interaction from the simulation ($25 \mu\text{m}$ sand particle)

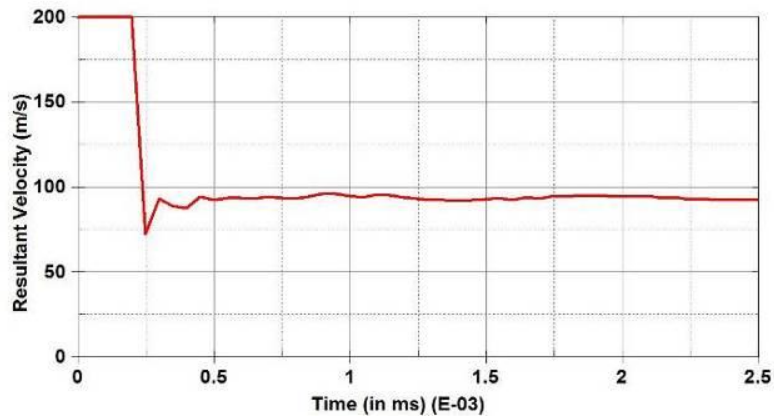


Fig. 8 Particle velocity change during surface interaction from the simulation ($25 \mu\text{m}$ sand particle)

Fig. 10 shows the particle velocity time history for a $50 \mu\text{m}$ diameter sand particle impact on TBC surface. This figure shows that with increased particle size, higher velocity change and hence higher kinetic energy is imparted on to the TBC surface. Fig. 11 shows the plastic strain on TBC surface due to a $50 \mu\text{m}$ diameter sand particle impact. Increased plastic strain levels are observed on the TBC surface from simulation as shown in Fig. 11.

Fig. 12 shows the particle impact model set-up for non-spherical 50 micron average sized sand particle with sharp edges as seen typically in the desert sand environment. The shape of the non-spherical particle was assumed as shown in Fig. 12, since natural sand comprises particles of random sizes and sharp edges. Fig. 13 shows the post-impact plastic strain on TBC with average 50 micron sized non-spherical (irregular) sand particle with sharp edges. Higher plastic strains within a small localized zone are observed on the TBC surface from simulation as shown in Fig. 13. Fig. 14 compares the resultant velocities of spherical and non-spherical (sharp-edged) 50 micron sand particles impacting with an initial velocity of 200 m/s. As seen in the Fig. 14, the non-spherical (sharp-edged) particle undergoes a greater velocity change resulting in higher impact energy transfer to the TBC surface, which indicates a more severe TBC surface damage with sharp-edged sand particles.

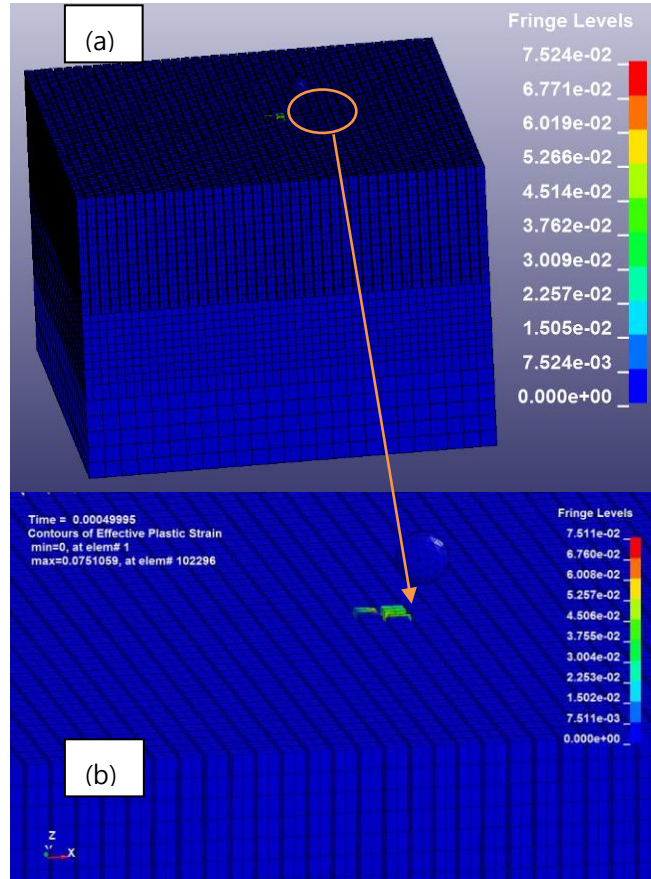


Fig. 9 Plastic strain contours on the TBC surface from the simulation (25 μm sand particle)

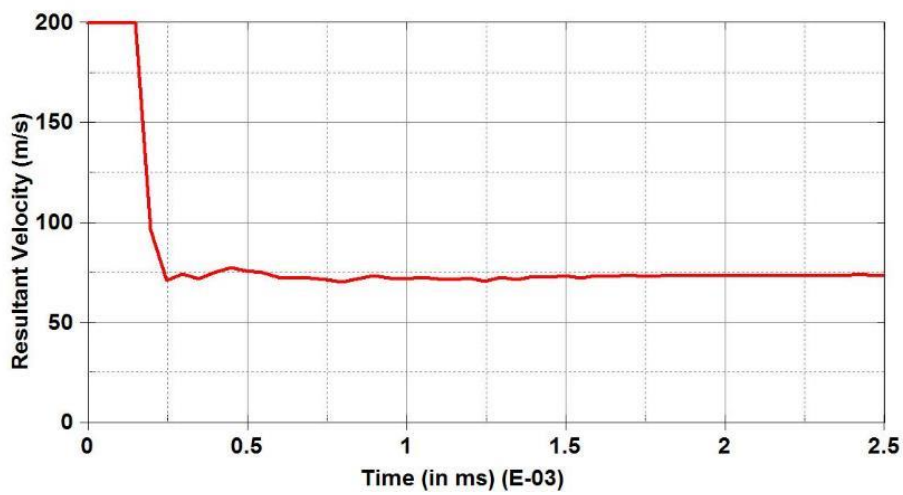


Fig. 10 Particle velocity change during surface interaction from the simulation (50 μm sand particle)

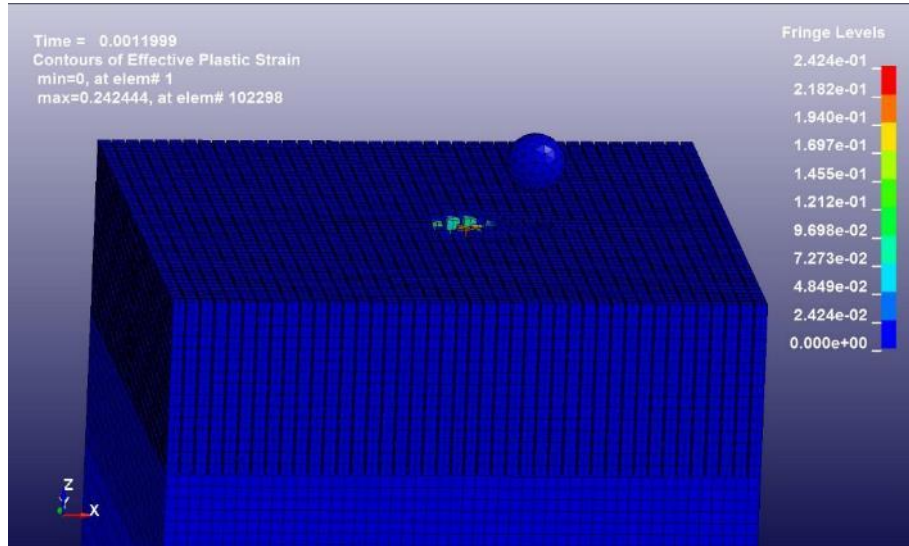


Fig. 11 Plastic strain contours on the TBC surface from the simulation (50 μm sand particle)

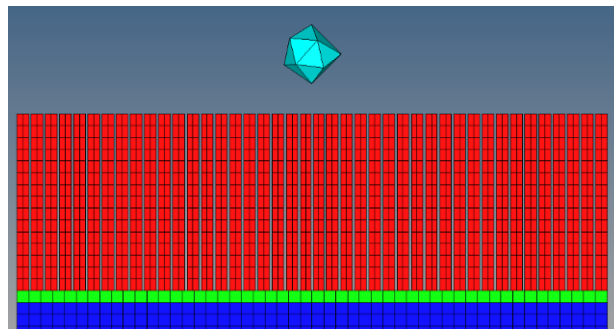


Fig. 12 50 micron average size non-spherical (irregular) sand particle with sharp edges (impact model)

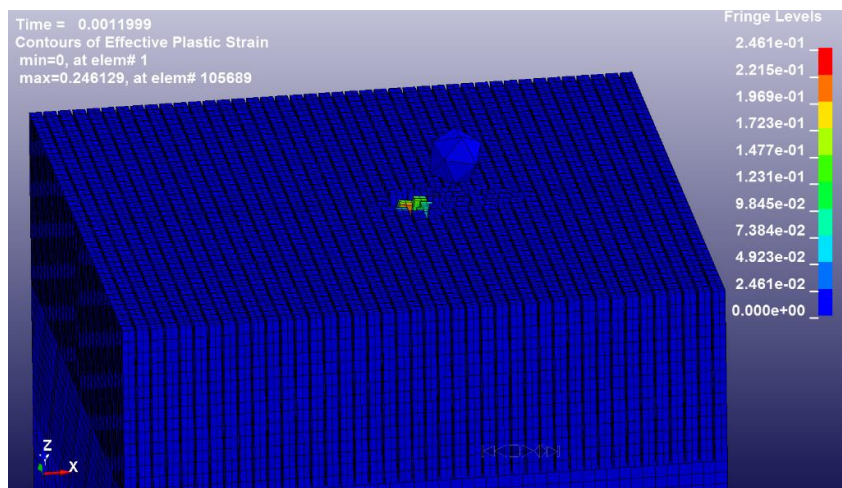


Fig. 13 Plastic strain on TBC with average 50 micron non-spherical (irregular) sand particle with sharp edges (post-impact)

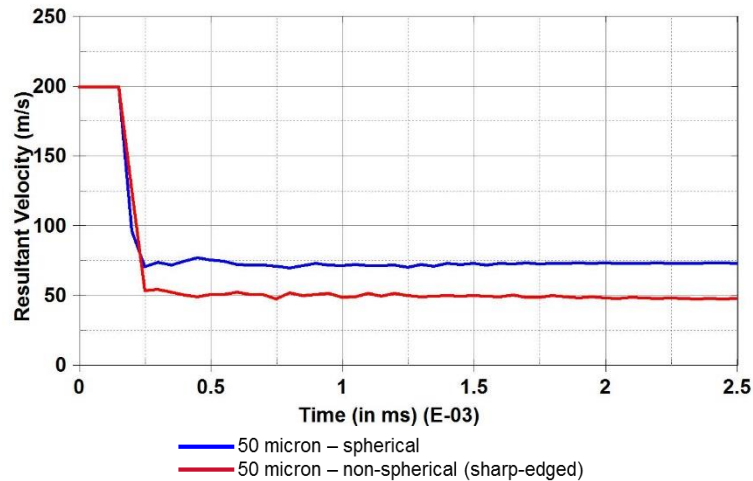


Fig. 14 Particle velocity change during particle-surface interaction-50 micron sand particle (spherical and non-spherical (sharp-edged))

3. Experimental efforts

3.1 Coating efforts

In order to validate and refine the aforementioned coating impact response models, candidate TBC materials will be consolidated and characterized. A variety of coating techniques will be used in order to fully characterize the effects of processing technology on the coating structure and ultimately mechanical response. Selected coatings will be subjected to jet burner erosion testing, with pre- and post-microstructural characterization to evaluate CMAS damage and impact resistance. Each coating technique provides a unique characteristic microstructure that can be evaluated independently of coating chemistry for the optimization of mechanical performance.

3.2 Air Plasma Spray (APS)

APS coatings are characterized by micron-scale splats of melted and re-solidified powder feedstock materials, micron-scale porosity, and micro-cracking at both particle-particle interfaces and interlaminar interfaces (Stöver, Pracht *et al.* 2004). APS typically produces coatings with reduced strain tolerance compared to Electron Beam Physical Vapor Deposition (EB-PVD) coatings; but will be used as a low cost, high throughput technique for initial screening and downselection of candidate TBC materials. The ability to quickly produce thick (100-300 micron) coatings in open air will be critical to reducing both the cost and time for evaluation of microstructural effects on coating properties, as well as the selection of ideal material candidates for use with other consolidation technologies.

3.3 Electron Beam Physical Vapor Deposition (EB-PVD)

EB-PVD is the current industry standard for TBCs, which are characterized by columnar

polycrystalline structures oriented normally to the substrate surface, with each column separated from its neighbors by small (approximately 2 micron) gaps (Jordan, Xie *et al.* 2004). Individual columns can also exhibit interior cracking across some or all of their width. These columns and cracks all serve to mediate thermal strains by reducing constraints during expansion and contraction of the superalloy substrate. Standard YSZ and downselected TBC materials will be consolidated by EB-PVD and microstructurally characterized both before and after jet burner sand ingestion testing. Microstructural and thermomechanical data will be used to validate and refine model parameters including EB-PVD column size, column spacing, and mechanical properties including adhesion strength and fracture toughness.

3.4 Solution Precursor Plasma Spray (SPPS)

SPPS is a recent development in thermal spray technology that allows for the reduction of APS microstructural feature size. SPPS uses the same plasma torch and consolidation process as APS, but a different feedstock and feeding mechanism. Instead of ceramic or metallic powders, solutions of coating precursor salts in solution are pumped in liquid suspensions to an atomizing nozzle, which directs droplets to the plasma torch (Killinger, Gadow *et al.* 2011). Once exposed to the heat of the plasma, they react to form the desired species. This process enables the formation and deposition of microstructures that show characteristics similar to both APS and EB-PVD, including pores and vertical cracking. However, due to the refined droplet size compared to the molten APS feedstock, the overall scale of the microstructure is much finer in SPPS than in APS. Peer reviewed studies show promising results for SPPS coating thermomechanical properties, including low thermal conductivity and enhanced wear resistance compared to APS and EB-PVD (Drexler, Aygun *et al.* 2010a).

3.5 Microstructural evaluation

All coatings will undergo microstructural evaluations before and after high temperature testing. This will reveal any significant changes in the coatings' structure and properties, due to high temperature and fine particle exposure. Results from these tests will be used to refine the multi-scale model of CMAS degradation. The evaluation will consist of:

- (a) Scanning electron microscopy to observe the physical microstructure,
- (b) Energy dispersive x-ray spectroscopy for compositional analysis,
- (c) X-ray diffraction to analyze the structure and stress states,
- (d) Confocal scanning acoustic microscopy to image the porosity and locate defects within the coatings,
- (e) Optical profilometry for studying the surface asperity,
- (f) Indentation testing to obtain information on the mechanical properties,
- (g) Thermal properties will be evaluated with several techniques, such as thermo-gravimetric analysis, thermo-(h) Mechanical analysis, and differential scanning calorimetry,
- (i) Other techniques will be used to characterize the coatings, as needed.

3.6 High-temperature testing

Evaluating the CMAS-attack resistance of the consolidated coatings will require unique tools. Specifically, a button cell flame testing rig and an atmospheric burner rig (with a sand/salt feeder

system) will be used. The button cell flame testing rig is a new apparatus (Fig. 15) that provides exposure to high temperatures in a relatively short amount of time, such as 3 minute hot/cold thermal cycling durations. This tool can assist in the down-selection of coating materials. Effectively, small samples (approximately 1-inch diameter) of TBC-coated superalloys will be placed in a stepper-motor controlled carousel. Samples will be thermally-cycled by rotating in and out of the flame. Typically, the coated samples are tested for three alternating thermal cycles of 3 minutes each with high temperature maintained at 1300°C (above sand melting point of 1250°C). The oxy-propane flame can be adjusted to accommodate a range of temperatures, up to approximately 2500°C. Sample surface temperatures will be measured via optical pyrometry and an infrared camera.

Once down-selected via the multi-scale model and experimental results with the button cell flame testing rig, new coatings can be tested in the modified jet burner rig. Using a JP8-air mixture, this test setup (Fig. 16) can reach temperatures in excess of 1500°C and hot air flow of up to ~0.8 Mach. Once fitted with a new sand/salt particle ingestion system, samples can be thermally-cycled in and out of the particle-laden jet exhaust and tested for CMAS-resistance.

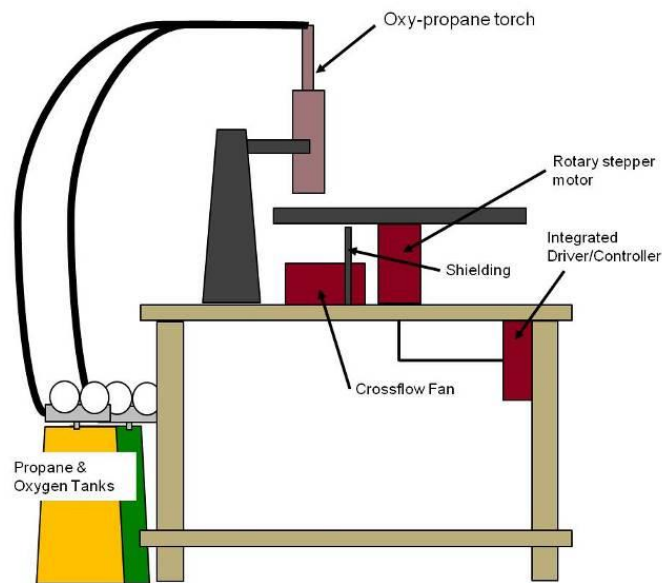


Fig. 15 Schematic of the button cell flame testing rig



Fig. 16 Jet burner rig

4. Conclusions

This paper outlines the efforts at ARL to research and develop effective thermal barrier coatings, which are resistant to CMAS-attack. At present, only a qualitative model is used to describe the attack and guide coating development. The details of the chemistry and physics involved in the attack process remain to be investigated. An initial dynamic mechanical impact model of a spherical, micrometer-sized sand particle impacting a columnar TBC has been developed. From this model, it has been concluded that:

- 1) A significant amount of the particle's kinetic energy is passed to the columnar TBC.
- 2) As a result, significant plastic strains from a single impact are observed on the TBC surface.
- 3) Multiple impacts may lead to strain build-up and the ultimate failure of the coating.
- 4) With increased particle size, higher kinetic energy is imparted to the TBC surface.
- 5) A sharp-edged non-spherical particle transfers a higher impact energy to the TBC surface as compared to a smooth spherical particle of the same size.

The information gained from this model will be used to guide the development of future computational efforts. Future modeling work will consist of adding fluid flow, thermodynamic effects, and chemical reactions between the TBC and the impinging sand particles. In addition to the modeling efforts, the U.S. Army Research Laboratory will pursue experiments to test current TBCs and internally developed innovative coatings for future possible replacements. The information collected will also guide, and eventually validate the models describing the complex interactions between impinging sand particles and the protective coatings used in the hot-sections of gas turbine engines.

Acknowledgments

The authors thank and acknowledge the inputs and suggestions for this research work from Dr. Jeffrey Swab, Dr. George Gazonas, Mr. Robert Dowding, and other research staff at the Weapons and Materials Research Directorate of the U.S. Army Research Laboratory, Aberdeen Proving Ground, Maryland, U.S.A.

References

- Aygun, A., Vasiliev, A.L., Padture, N.P. and Ma, X. (2007), "Novel thermal barrier coatings that are resistant to high-temperature attack by glassy deposits", *Acta Materialia*, **55**, 6734-6745.
- Borom, M.P., Johnson, C.A. and Peluso, L.A. (1996), "Role of environment deposits and operating surface temperature in spallation of air plasma sprayed thermal barrier coatings", *Surf. Coat. Technol.*, **86**, 116-126.
- Drexler, J., Aygun, A., Li, D., Vaßen, R., Steinke, T. and Padture, N.P. (2010a), "Thermal-gradient testing of thermal barrier coatings under simultaneous attack by molten glassy deposits and its mitigation", *Surf. Coat. Technol.*, **204**, 2683-2688
- Drexler, J.M., Shinoda, K., Ortiz, A.L., Li, D., Vasiliev, A.L., Gledhill, A.D., Sampath, S. and Padture, N.P. (2010b), "Air-plasma-sprayed thermal barrier coatings that are resistant to high-temperature attack by glassy deposits", *Acta Materialia*, **58**, 6835-6844.
- Evans, A.G., Mumm, D.R., Hutchinson, J.W., Meier, G.H. and Pettit, F.S. (2001), "Mechanisms controlling

- the durability of thermal barrier coatings”, *Progress in Materials Science*, **46**, 505-553.
- Hamed, A. (1988), “Effect of particle characteristics on trajectories and blade impact patterns”, *J. Fluid. Eng.*, **110**, 33-37.
- Hutchinson, J.W. and Evans, A.G. (2002), “On the delamination of thermal barrier coatings in a thermal gradient”, *Surf. Coat. Technol.*, **149**, 179-184.
- Jordan, E.H., Xie, L., Ma, X., Gell, M., Padture, N.P., Cetegen, B., Ozturk, A., Roth, J., Xiao, T.D. and Bryant, P.E.C. (2004), “Superior thermal barrier coatings using solution precursor plasma spray”, *J. Therm. Spray Tech.*, **13**(1), 57-65.
- Killinger, A., Gadow, R., Mauer, G., Guignard, A., Vaßen, R. and Stöver, D. (2011), “Review of new developments in suspension and solution precursor thermal spray processes”, *J. Therm. Spray Tech.*, **20**(4), 677-695.
- Kramer, S., Yang, J. and Levi, C.G. (2008), “Infiltration-inhibiting reaction of gadolinium zirconate thermal barrier coatings with CMAS melts”, *J. Am. Ceramic Soc.*, **91**, 576-583.
- Levi, C.G., Hutchinson, J.W., Vidal-Setif, M.H. and Johnson, C.A. (2012), “Environmental degradation of thermal-barrier coatings by molten deposits”, *MRS Bull*, **37**, 932-941.
- LSTC (2007), *LS-DYNA Keyword User’s Manual, Version 971*, Volume I, May, Livermore Software Technology Corporation (LSTC), Livermore, CA.
- Murugan, D.M., Tabakoff, W. and Hamed, A. (1994), “Computation of particle restitution characteristics using DYNA3D for turbomachinery application”, *30th AIAA/ASME/SAE/ASEE Joint Propulsion Conference*, Indianapolis, Indiana, June.
- Padture, N.P., Gell, M. and Jordan, E. H. (2002), “Thermal barrier coatings for gas-turbine engine applications”, *Science*, **296**, 280-284.
- Rai, A.K., Bhattacharya, R.S., Wolfe, D.E. and Eden, T.J. (2010), “CMAS-resistant thermal barrier coatings”, *Int. J. Appl. Ceramic Tech.*, **7**, 662-674.
- Smialek, J.L., Archer, F.A. and Garlick, R.G. (1994), “Turbine airfoil degradation in the Persian Gulf war”, *JOM*, **46**, 39-41.
- Stöver, D., Pracht, G., Lehmann, H., Dietrich, M., Dö ring, J.E. and Vaßen, R. (2004), “New material concepts for the next generation of plasma-sprayed thermal barrier coatings”, *J. Therm. Spray Tech.*, **13**(1), 76-83.
- Tabakoff, W. (1991), “Measurements of particles rebound characteristics on materials used in gas turbines”, *J. Propuls.*, **7**(5), 805-813.
- Tabakoff, W., Murugan, D.M. and Hamed, A. (1994), “Effect of target materials on the particle restitution characteristics for turbomachinery application”, *32nd Aerospace Sciences Meeting & Exhibit*, Reno, Nevada, January.

EC

Nomenclature

APS	=	Air Plasma Spray
ARL	=	Army Research Laboratory
BSAS	=	Barium Strontium Aluminum Silicate
CMAS	=	Calcium-Magnesium-Alumina-Silicate
CMC	=	Ceramic Matrix Composite
CFD	=	Computational Fluid Dynamics
CTE	=	Coefficient of Thermal Expansion
DFT	=	Density Functional Theory

EB-PVD	=	Electron Beam Physical Vapor Deposition
EBC	=	Environmental Barrier Coating
m/s	=	meters per second
μm	=	micrometer
ms	=	milliseconds
MD	=	Molecular Dynamics
SiC	=	Silicon Carbide
SPPS	=	Solution Precursor Plasma Spray
SWA	=	Southwest Asia
TBC	=	Thermal Barrier Coating
TGO	=	Thermally Grown Oxide
YSZ	=	Yttria Stabilized Zirconia